JOURNAL OF SOLID STATE CHEMISTRY 40, 8–13 (1981)

Crystalline Structure and OH Torsional Motion in Calcium–Strontium Arsenate Apatites

P. F. GONZÁLEZ-DÍAZ AND PRISCILA GARCÍA-FERNÁNDEZ

Instituto de Optica "Daza de Valdés," CSIC, Serrano 121, Madrid-6, Spain

Received December 9, 1980; in revised form April 10, 1981

The crystalline structure of $Ca_{10-x}Sr_x(AsO_4)_6(OH)_2$ has been studied, and the lattice parameters determined. It has been found that the unit cell expands with x. Geometric parameters of the unit cell, which are defined in relation to the hindered rotation of the OH group around the c axis, have been also obtained. From the ir data, the torsional potential function has been calculated in first and second approximations. A method for computing that function in any order approximation is given. A semiempirical curve is found, relating the stretching and torsional motions for both the OH and OD groups.

Introduction

The ir spectra of the calcium–strontium arsenate apatites have been already studied (*1*). It is seen (*1*) that Ca and Sr undergo *continuous ordered migrations* throughout the crystal, in a way similar to that suggested by Heijhgers *et al.* (*2*) and by Andrés-Verges *et al.* (*3*) in calcium–strontium phosphate apatites. We give X-ray data in this paper confirming that suggestion. On the other hand, the torsional motion of the OH and OD groups is studied using the ir results reported in Ref. (*1*). The torsional potential function is theoretically discussed in some detail, the relation existing between the torsional and stretching motions being of particular interest.

Experimental

The synthesis of the compounds $Ca_{10-x}Sr_x(ASO_4)_6(OH)_2$ was made following the method described in Ref. (*1*). Infrared absorption spectra were recorded on a Perkin–Elmer 599 B spectrophotometer. X-Ray diffractograms were obtained with a Philips PW1130/00 (generator) and a PW1050/25 goniometer with a Cu anticathode (40 kV, 20 mA).

Deuterated analogs were prepared by treating the samples on an inert plate with excess D_2O vapor in a glass cell at 350°C for 4 hr.

Results and Discussion

(*a*) *X-Ray data*

From the diffraction patterns (*1*) corresponding to $Ca_{10-x}Sr_x(AsO_4)_6(OH)_2$, for x = 1, 2, . . ., 9, we have determined the spacing and relative intensities associated with all the reflections between 2 and 40°. As an example, we give in Table I these data for x = 5. For the sake of precision we have used TlCl as a reference in all our measurements. It can be observed that the spacings become larger as the Sr proportion in the crystal increases.

It has been suggested (*1–3*) that the

0022-4596/81/130008-06$02.00/0

TABLE I

SPACINGS AND RELATIVE INTENSITIES OF THE DIFFRACTION PATTERN FOR $x = 5$

hkl	d (Å)	I/I_{max}
100	8.6818	0.07
111	4.1257	0.06
002	3.6508	0.29
210	3.2616	0.21
211	2.9770	1.00
112	2.9397	0.60
300	2.8750	0.54
202	2.7851	0.12
310	2.3901	0.07
221	2.3551	0.04
311	2.2713	0.07

cations in calcium–strontium apatites continuously interchange their respective positions, so that each cation site is occupied by an "effective cation," whose properties are an average over the properties of all the cations present in the unit cell.

The hexagonal (*4–8*) lattice parameters for all the samples are plotted in Fig. 1 vs the composional parameter x. It can be observed that for low values of x ($x < 4$), all of them expand with x more rapidly along the c axis, so confirming what was suggested from the ir data (*1*).

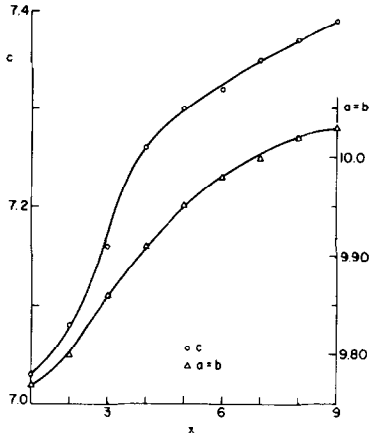

FIG. 1. Variations of the hexagonal cell parameters vs x.

The OH groups bond to the nearest oxygens of the surrounding anions through linear hydrogen bonds (*9, 10*) so that the distances $O-H \cdots OAsO_3$, d have been calculated making use of the recorded $\nu_s(OH)$ frequencies (*8*). Results are given in Table II. It is noted that d increases with x, except for $x = 6$ and 7. When this fact is compared with the X-ray data discussed above, one can conclude that the positions of the OH groups along the c axis are rather random.

Geometric parameters of the unit cell characterizing the hindered rotation of the

TABLE II

GEOMETRICAL PARAMETERS OF THE UNIT CELL CHARACTERIZING THE TORSIONAL MOTION OF THE OH GROUP AROUND THE c AXIS, AND DYNAMICAL PARAMETERS FOR THE OH TORSIONAL MOTION

x	d (Å)	r (Å)	S (Å)	cos α	y (Å)	I_r (10^{-40} g · cm^2)	T (cm^{-1})
1	3.07	2.97	0.65	0.967	0.972	1.568	17.84
2	3.10	2.98	0.59	0.963	0.966	1.549	18.05
3	3.10	3.01	0.71	0.973	0.976	1.581	17.69
4	3.14	3.04	0.64	0.968	0.969	1.559	17.94
5	3.14	3.06	0.72	0.974	0.975	1.578	17.72
6	3.12	3.07	0.90	0.986	0.987	1.617	17.29
7	3.12	3.08	0.96	0.989	0.990	1.627	17.19
8	3.16	3.09	0.79	0.979	0.979	1.591	17.58
9	3.17	3.10	0.77	0.978	0.958	1.523	18.36

TABLE III

OPTIMUM VALUES OF THE TORSIONAL BARRIER CALCULATED BY BOTH THE PROGRAM (V_3) AND THE HARMONIC APPROXIMATION (V_3^h)

x	V_3 (cm^{-1})	V_3^h (cm^{-1})
1	2750	2433
2	2635	2291
3	2555	2224
4	2293	1977
5	2275	1966
6	2335	2030
7	2345	2042
8	2370	2053
9	2294	1980

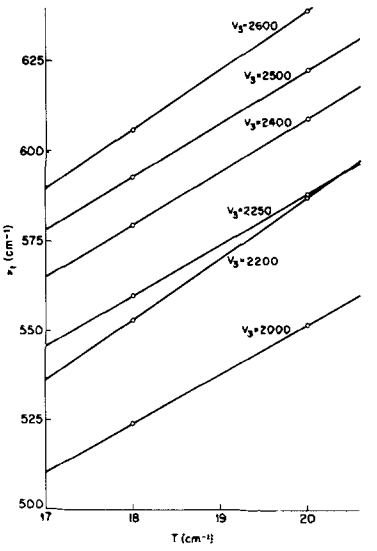

FIG. 3. ν_t(OH) vs T for different values of V_3.

OH group around the c axis are represented in Fig. 2. From the data given in Table II and using a curve relating ν_s(OH) vs the O–H distances (*10*), we have computed those geometric parameters (Table II). In Table III are also given the reduced moment of inertia of the OH rotor ($I_r = m_H y^2$) and its related OH torsional constant ($T(cm^{-1}) = h^2/8\,\pi^2 c I_r$, h being the Planck's constant, and c the velocity of light in vacuum).

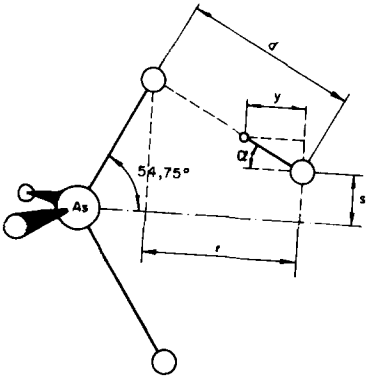

FIG. 2. Geometric parameters of the unit cell with respect to the hindered rotation of the OH group around the x axis.

(b) Torsional Motion of the OH groups

The OH torsional potential function in first order approximation is (*11*):

$$V(\phi) = V_3/2\,(1 - \cos 3\phi), \qquad (1)$$

where ϕ is the rotation angle and V_3, the rotation barrier, is threefold as it corresponds to the three equivalent hydrogen bonds $HO \cdots OAsO_3$ that the OH forms along a complete rotation around the c axis.

Making use of a Fortran IV program (*10, 12*), we have obtained the optimized

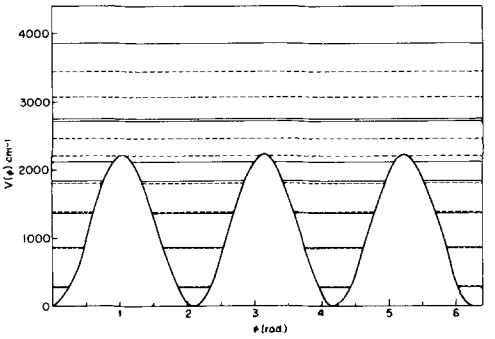

FIG. 4. Torsional potential function in first-order approximation, and energy levels for $x = 4$.

TABLE IV

TRANSMISSION COEFFICIENTS OF THE BARRIERS $V_3(\phi)$

	τ		
Wavefunction[a]	$0 \rightarrow 2\pi/3$	$2\pi/3 \rightarrow 4\pi/3$	$4\pi/3 \rightarrow 0$
ψ_2^e	0.25	1	
ψ_2^o	0	1	0
ψ_3^e	0	1	0
ψ_3^o	0.50	1	
ψ_6^e	0.79	1	
ψ_6^o	0	1	
ψ_7^e	0.87	1	
ψ_7^o	0.25	1	

[a] ψ^e: ψ even, ψ^o: ψ odd.

values of the barrier V_3 (Table III), the torsional energy levels, and their associated wave functions. The values of V_3 calculated from the harmonic approximation of the potential (*2, 13*) are also given in Table III ($V_3^h = \nu_t^2/9T$). Using the program, we have also built up the curves $\nu_t = \nu_t(T)$ for different values of V_3 (Fig. 3). Hence, functions $\nu_t = \nu_t(V_3)$ may be constructed and the optimized V_3 values computed for any value of x, following the same method as used above (*10, 12*). In Table III only the V_3 values corresponding to integer values of x are given.

TABLE V

OPTIMUM VALUES OF THE OD TORSIONAL BARRIER CALCULATED BY BOTH THE PROGRAM (V_3) AND THE HARMONIC APPROXIMATION (V_3^h)

x	$V_3^{(h)}$ (cm^{-1})	V_3 (cm^{-1})	$V_3 - V_3^{(h)}$ (cm^{-1})
1	2523	2725	202
2	2373	2615	242
3	2302	2520	218
4	2051	2271	220
5	2036	2255	219
6	2097	2305	208
7	2110	2305	195
8	2125	2333	208
9	2050	2274	224

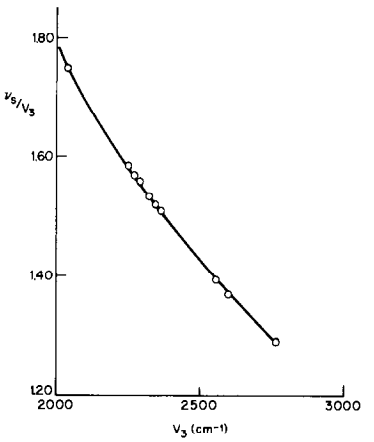

FIG. 5. ν_s/V_3 vs V_3 for the group OH.

In Fig. 4, we give as an example, the potential function ($V_3 = 2293\ cm^{-1}$) and the energy levels for $x = 4$. The levels with discontinuous lines correspond to doubly degenerate levels. It can be observed that the degeneracy possesses a certain periodicity, which originates from the C_3 symmetry of the potential function. On the other hand, for $E \leq V_3$ the separation between energy levels gets smaller, whereas for $E > V_3$ the behavior of that separation gets larger, as is the case of a free rotor.

Taking into account the C_3 symmetry of the potential function, we have found that the wavefunctions corresponding to nonde-

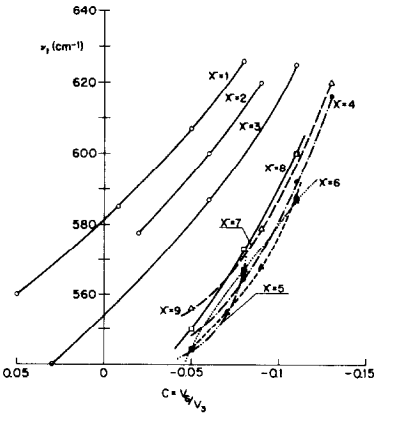

FIG. 6. ν_t(OH) vs $C = V_6/V_3$ for all cases.

TABLE VI

OPTIMUM VALUES OF V_3, $C = V_6/V_3$, AND V_6

x	V_3	C	V_6
1	3578	−0.08	−286
2	3572	−0.075	−245
3	3159	−0.074	−234
4	2908	−0.08	−233
5	2858	−0.078	−223
6	2883	−0.074	−213
7	3020	−0.081	−245
8	2985	−0.078	−233
9	3018	−0.086	−260

generate levels belong to the species A, and the remainder belong to the doubly degenerate species E. The transmission coefficients, τ, associated with some wavefunctions are given in Table IV. It is worth noting that $\tau = 1$ for wavefunctions belonging to the A species.

Using the recorded ν_t(OD) frequencies (*1*), and assuming $T(\text{OD}) = \frac{1}{2}\ T(\text{OH})$, we have calculated the OD torsional barriers by means of both the Fortran IV program (V_3) and the harmonic approximation procedure (V_3^h). Values are given in Table V. The shifts $\Delta V_3 = V_3 - V_3^h$ are smaller for OD than for OH, provided that the V_3 (OD) values are lower than the V_3 (OH).

The influence of the strength of the hydrogen bond OH· · ·$OAsO_3$ (which must relate directly to V_3 on the OH stretching frequency ν_s) is displayed in Fig. 5. The semi-empirical curve in this figure can be represented by the equation:

$$\nu_s = 2.68 \times 10^{-7}\ V_3^3 - 1.93 \times 10^{-3}\ V_3^2 + 4.56\ V_3. \quad (2)$$

This relation shows that Oswald's law (*10*) does not hold true for calcium–strontium apatites. A similar curve has been found for the OD case.

The torsional potential function developed to a second-order approximation is:

$$V(\phi) = V_3/2\ (1 - \cos 3\phi) + V_6/2\ (1 - \cos 6\phi). \quad (3)$$

From the harmonic approximation (*13*), one has:

$$\nu_t^2/T = 9V_3 + 36V_6. \quad (4)$$

To obtain the coefficients V_3 and V_6, we have proceeded as follows: Different couples (V_3, V_6) satisfying Eq. (4) for the experimental ν_t have been tested in the program for each value of x, thus obtaining curves $\nu_t = \nu_t(C)$, (C being the ratio V_3/V_6), which are given in Fig. 6. Carrying the experimental values of ν_t into these curves, optimum values of C have been found for each case. Then, using Eq. (4), we have determined the optimum values of couples (V_3, V_6), which are given in Table VI. It can be observed that the values of V_3, V_6, and C are rather random with respect to x, such as happened with V_3 in the first approximation. Since all V_6 are small and negative, the effect of V_6 on the shape of the potential function is to make the well slightly broader.

It is worth noting that the method used to obtain two terms in the torsional potential function can be extended to any higher-order approximation.

Acknowledgment

The writers are indebted to Dr. A. Hernández-Laguna of the Instituto Geológico y Minero, Madrid, for the recording of the X-ray diffraction patterns.

References

1. P. GARCÍA-FERNÁNDEZ AND P. F. GONZÁLEZ-DÍAZ, *Spectrochim. Acta A*, **36**, 1069 (1980).
2. H. J. M. HEIJHGERS, R. M. H. VERBEECK, AND F. C. M. DRIESSENS, *J. Inorg. Nucl. Chem.* **41**, 763 (1979).
3. M. ANDRÉS-VERGES, F. J. HIGES, AND P. F. GONZÁLEZ-DÍAZ, *J. Solid State Chem.* **33**, 125 (1980).
4. A. S. POSNER, A. PERLOFF, AND A. F. DIORIO, *Acta Crystallogr.* **11**, 308 (1958).

5. M. A. KAY AND R. A. YOUNG, *Nature* **204,** 1050 (1964).
6. R. J. HANWICK AND P. HOFFMAN, *J. Chim. Phys.* **17,** 1166 (1949).
7. R. E. RUNDLE AND M. PARASOL, *J. Chim. Phys.* **20,** 1487 (1952).
8. M. J. BUERGER, "X-Ray Crystallography." Wiley, New York (1942).
9. J. C. ELLIOT, *J. Dent. Res.* **41,** 1251 (1962).
10. P. F. GONZÁLEZ-DÍAZ AND M. SANTOS, *J. Solid State Chem.* **22,** 193 (1977).
11. C. C. LIN AND J. D. SWALEN, *Rev. Mod. Phys.* **31,** 841 (1959).
12. P. F. GONZÁLEZ-DÍAZ AND A. HIDALGO, *Spectrochim. Acta A* **32,** 1119 (1976).
13. W. A. FATELEY, R. K. HARRIS, F. A. MILLER, AND R. E. WITKOWSKI, *Spectrochim. Acta* **21,** 231 (1965).